Physica E 67 (2015) 18–22

Contents lists available at ScienceDirect

Physica E

journal homepage: www.elsevier.com/locate/physe

# Enhanced photocatalytic performance of $TiO_2$ particles via effect of anatase–rutile ratio

N. Yuangpho [a], S.T.T. Le [a], T. Treerujiraphapong [a,b], W. Khanitchaidecha [a,c], A. Nakaruk [b,d,*]

[a] Centre of Excellence for Innovation and Technology for Water Treatment, Naresuan University, Phitsanulok 65000, Thailand
[b] Department of Industrial Engineering, Faculty of Engineering, Naresuan University, Phitsanulok 65000, Thailand
[c] Department of Civil Engineering, Faculty of Engineering, Naresuan University, Phitsanulok 65000, Thailand
[d] Center of Excellence for Environmental Health and Toxicology, Naresuan University, Phitsanulok 65000, Thailand

## HIGHLIGHTS

- Comprehensive investigation on anatase–rutile phase transformation.
- Phase composition ratio can be controlled through annealing temperature.
- The effect of annealing temperature on physical and chemical properties were intensively investigated.
- The photocatalysis efficiency of $TiO_2$ particles were evaluated.
- The results indicated the advantages of mixed phase anatase–rutile on photocatalysis mechanism.

## ARTICLE INFO

*Article history:*
Received 4 August 2014
Received in revised form
21 October 2014
Accepted 11 November 2014
Available online 13 November 2014

*Keywords:*
Titanium dioxide
Anatase
Rutile
Phase transformation
Photocatalytic

## ABSTRACT

In the present work anatase–rutile transformation temperature and its effect on physical/chemical properties as well as photocatalytic activity of $TiO_2$ particles were investigated. The characterisation of the synthesised and annealed $TiO_2$ particles were determined by X-Ray Powder Diffraction (XRD), scanning electron microscope (SEM), dynamic light scattering (DLS) and Brunauer–Emmett–Teller surface area analysis (BET). The refraction in the ultraviolet–visible (UV–vis) range was assessed using a dual-beam spectrophotometer. The photocatalytic performance of the particles was tested on methylene blue solution. The XRD data indicated that the percentage of rutile increased with the annealing temperature and almost 100% of anatase transformed to rutile at 1000 °C. In addition, the phase transformation was a linear function of annealing temperature so phase composition of $TiO_2$ can be controlled by changing the annealing temperature. The SEM and BET results presented the increase of agglomerate size and the decrease of specific surface area with the increasing annealing temperature. This proved that anatase has smaller particle size and higher surface area than rutile. The photocatalytic activity of the annealed $TiO_2$ powders reduced with the increase of annealing temperature. The samples annealed at 900 °C and 925 °C with anatase: rutile ratio of 92:8 and 77:23, respectively, showed the best activity. These results suggested that the photocatalytic activity of $TiO_2$ particles is a function of phase composition. Thus it can be enhanced by changing its phase composition which can be controlled by annealing temperature.



## 1. Introduction

At the present time, titanium dioxide ($TiO_2$) has been commercially used in many applications including, dye synthesised solar cells (DSSCs) [1], water splitting [2], self-cleaning [3], and water purification [4] due to its strong oxidising behaviour, good photocatalytic activity, chemical stability, and non-toxicity. Naturally, $TiO_2$ can be found in three polymorphs including, anatase, rutile and brookite [5]. In general, anatase and rutile are the most important and studied polymorphs. Anatase is stable at low temperature and known to have small grain sizes, resulting higher surface areas and low surface energy [6–8]. Owing to mentioned advantages, anatase is widely used for photocatalysis applications. However, it has to be noted that anatase is a wide band gap semiconductor with 3.2 eV of band gap [9]. This means it the activity can be active under only ultraviolet (UV) radiation. On the

* Corresponding author at: Department of Industrial Engineering, Faculty of Engineering, Naresuan University, Phitsanulok 65000, Thailand.
*E-mail address:* auppathamn@nu.ac.th (A. Nakaruk).

http://dx.doi.org/10.1016/j.physe.2014.11.006
1386-9477/

other hands, rutile has lower band gaps with ~3.0 eV [10] but the large grain size and high electron–hole recombination rate are disadvantage of rutile [11]. Alternatively, the combination of mixed phase anatase–rutile has been introduced in order to resolve the limitation of sole phase of $TiO_2$. The state of the art articles [12–14] suggest that mixed phase of anatase–rutile can enhance the photocatalytic performance. Kafizas et al. [15] mentioned that the combination of two phase can enhance electron–hole separation and extend the decrease band gap, which allows photocatalysis mechanism can be active under both UV and visible light.

Theoretically, anatase transform to rutile ~600 °C [16]. However, the transformation temperature of anatase → rutile has been reported to vary between 400 °C and 900 °C [12,17,18]. Therefore, the intentions of the present work were to 1) investigate the anatase–rutile transformation temperature, 2) examine the effect of annealing temperature on physical and chemical properties of $TiO_2$ particle, and 3) evaluate the photocatalytic performance of $TiO_2$ particles with difference anatase–rutile ratio.

## 2. Methodology

The anatase powder (Sigma-Aldrich, 99%) was used as starting materials, called commercial anatase. It consisted of 96% of anatase and 4% of rutile, as shown in Table 1. The mixed phase of anatase and rutile was synthesised by annealing the commercial anatase in muffle furnace at different temperature. Commercial anatase was put into alumina crucible and annealed in the muffle furnace with 3 °C/min of heating rate in air for 6 h, followed by natural cooling. The annealing temperatures were 900, 925, 950, 975, and 1000 °C.

The phase composition was determined by X-Ray Powder Diffraction (XRD, Panalytical *Expert*). The morphology of powders were analysed using scanning electron microscope (SEM, JEOL *JEM2010*). Agglomerate size of $TiO_2$ particles and specific surface area were examined using dynamic light scattering (DLS, Malvern Instruments *Zetasizer Nano-ZS*) and Brunauer–Emmett–Teller surface area analysis (BET, Horiba *SA*-9600), respectively. The refraction in the ultraviolet–visible (UV–vis) range was assessed using a dual-beam spectrophotometer with integrating sphere (Perkin-Elmer *Lambda 35*). The optical indirect band gap was calculated from these data using the method of Tauc and Menth [19]. The photocatalytic activity was analysed in terms of the degradation of methylene blue (MB) solution under irradiation (36 W) of UV light (380 nm) in ambient conditions (25 °C, atmospheric pressure). The MB solution of $1 \times 10^{-5}$ M concentration [20] was prepared using methylene blue (Regent Plus, Sigma-Aldrich) dissolved in de-ionised (DI) water. The solution was kept in a dark box in order to avoid any degradation from sunlight. $TiO_2$ powders were put in the solution for 2 h before testing in order to avoid the MB absorption on the surface.

**Table 1**
Summary of analytical data.

| Samples | Anatase (vol%) | Rutile (vol%) | Agglomerate size of $TiO_2$ particles (nm) | Specific surface area ($m^2$/g) | Band gap (eV) |
|---|---|---|---|---|---|
| Commercial anatase | 95.97 | 4.03 | 400 | 9.73 | 3.74 |
| 900 °C | 91.50 | 8.50 | 647 | 6.60 | 3.70 |
| 925 °C | 76.92 | 23.08 | 791 | 5.33 | 3.64 |
| 950 °C | 49.37 | 50.63 | 905 | 3.93 | 3.42 |
| 975 °C | 20.00 | 80.00 | 949 | 3.09 | 3.35 |
| 1000 °C | 2.17 | 97.83 | 1013 | 2.94 | 3.32 |

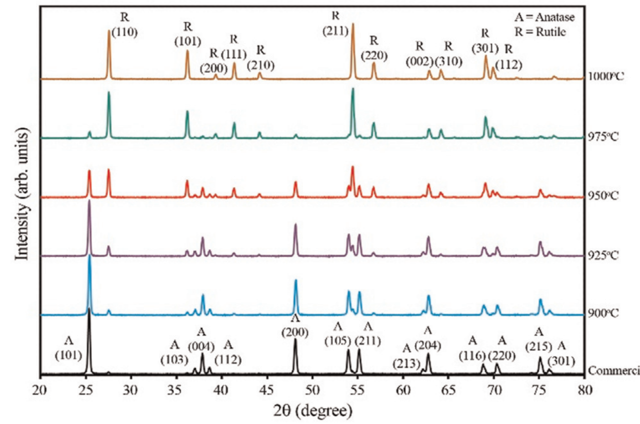


**Fig. 1.** XRD patterns of the commercial anatase and annealed $TiO_2$ powders at different temperatures.

## 3. Results and discussion

### 3.1. Particles characterisation

Fig. 1 shows the XRD patterns of the commercial anatase and annealed $TiO_2$ powders. It has to be noted that the commercial anatase consisted of both anatase (96 vol%) and rutile (4 vol%) phases. The volume percentages of anatase and rutile phase can be obtained from the ratio of peak intensities as given by [21]:

$$\frac{I_a}{I_r} = \frac{e^{-\mu_a \rho_a}}{e^{-\mu_r \rho_r}}$$

Where:

$I_a$ = peak intensity of anatase
$I_r$ = peak intensity of rutile
$\mu_a$ = mass absorption coefficient of anatase (129.41 $cm^2$/g [22]
$\mu_r$ = mass absorption coefficient of rutile (138.87 $cm^2$/g [22]
$\rho_a$ = true density of anatase (3890 kg/$m^3$ [22])
$\rho_r$ = true density of rutile (4250 kg/$m^3$ [22])

The result from calculation is shown in Table 1. The XRD patterns and calculated data indicate that the percentage of rutile increases with the annealing temperature. It can be seen that at 1000 °C of annealing temperature, anatase powders almost transform to rutile.

The plot of rutile percentage versus annealing temperature is shown in Fig. 2. The ratio of anatase to rutile at 900 °C is 92:6, which is comparable to the commercial anatase. The percentage of crystalline transformation from anatase to rutile is approximately 50% at 950 °C and almost complete (~100%) at 1000 °C. It is clearly indicated that the phase transformation is a linear function of annealing temperature. These data suggests that the phase composition can be controlled through the annealing process. In the other words, it is possible to synthesise $TiO_2$ powder with expected anatase and rutile ratio based on controlling the annealing temperature.

In general, anatase transform to rutile at 600 °C. However, it is very well known that this mechanism can be affected by contamination. Some impurities are known to inhibit the mechanism, Al is one of inhibitor [23]. Hanaor and Sorrell [23] reported that Al can extend the anatase–rutile phase transformation temperature. Since the particle was placed in alumina crucible, this means Al from crucible can be diffuse into the particles and inhibit the phase transformation.

Fig. 3 shows the SEM images of the commercial anatase and annealed $TiO_2$ powders. The images suggest that the agglomerate

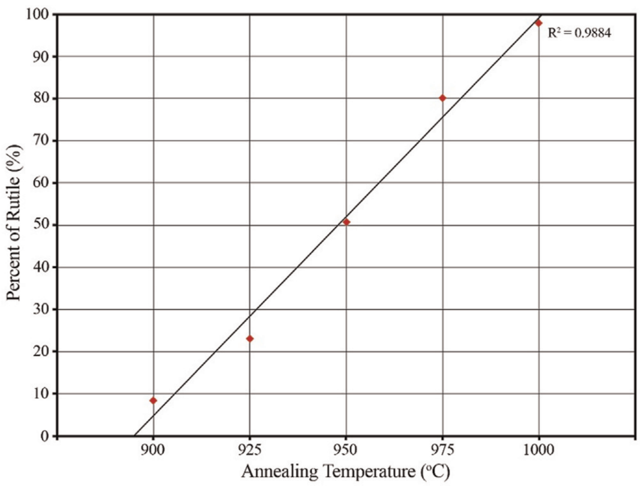


**Fig. 2.** Percentage of rutile phase as a function of annealing temperatures.

size of $TiO_2$ particle increased with increasing annealing temperature. Small particles of anatase agglomerate to be large particles of rutile, result to increasing of agglomerate size. These results are supported by BET and DLS data, which are shown in Fig. 4. These data clearly proves that the agglomerate size of $TiO_2$ particles of commercial anatase (~400 nm) increased to 1000 nm of rutile (annealed at 1000 °C). In the meantime, the specific surface area of commercial anatase particles decreased significantly from 9.80 $m^2/g$ to 2.9 $m^2/g$ with the increasing of annealing temperature to 1000 °C. It has to be note that the specific surface area of the commercial anatase is ~1 $m^2/g$, which is relatively higher than the annealed particles. These observations can be explained by the agglomeration of particles at high annealing temperature, which result in the increase of agglomerate size and the decrease of specific surface area. The same phenomenon has been reported in other studies [12,13]. These results are also in agreement with the idea that anatase has the smaller particle size and higher specific surface area compared to rutile.

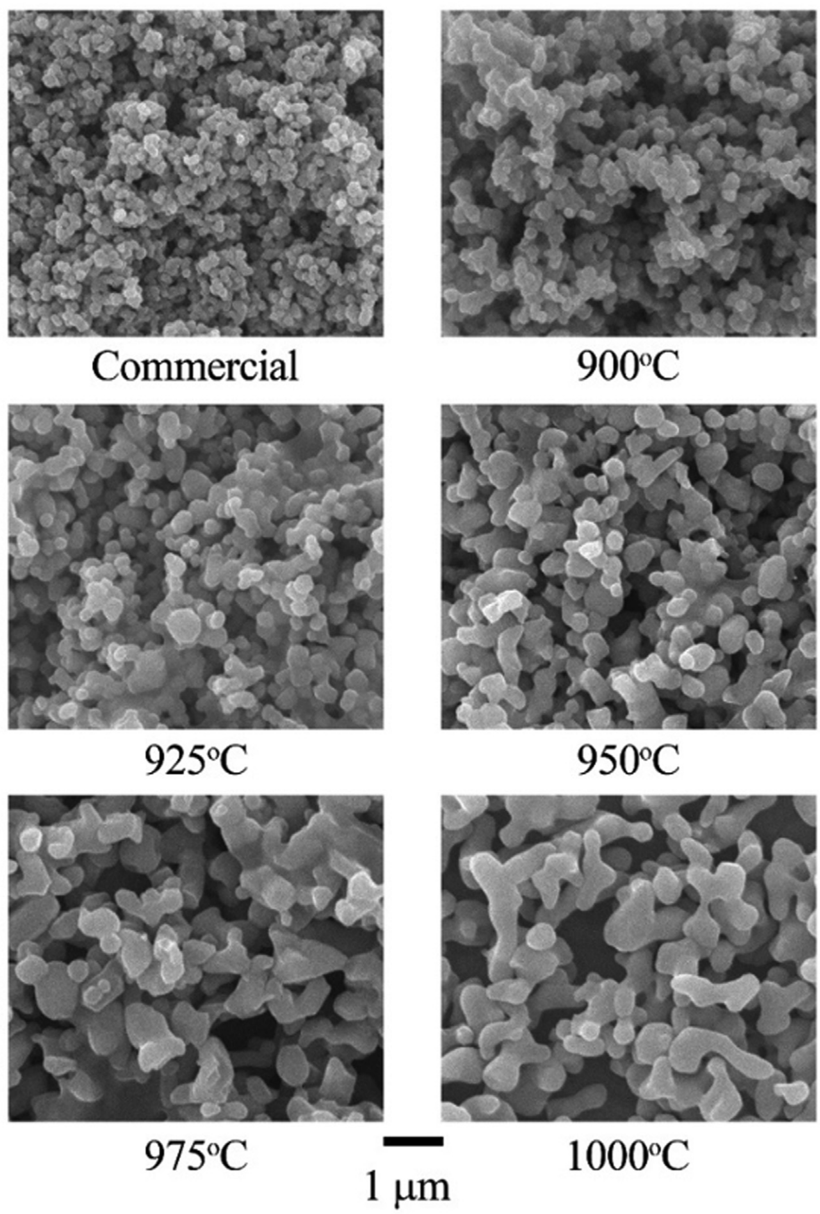


**Fig. 3.** SEM images of the commercial anatase and annealed $TiO_2$ powders at different temperatures.

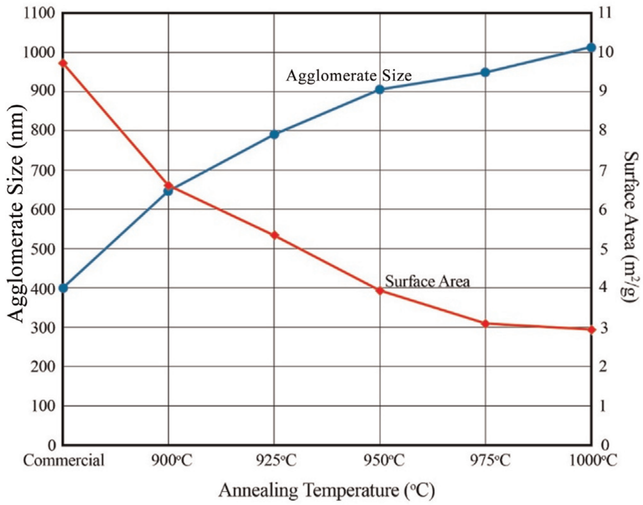


**Fig. 4.** The agglomerate size and specific surface area of the commercial anatase and annealed $TiO_2$ powders as a function of annealing temperature.

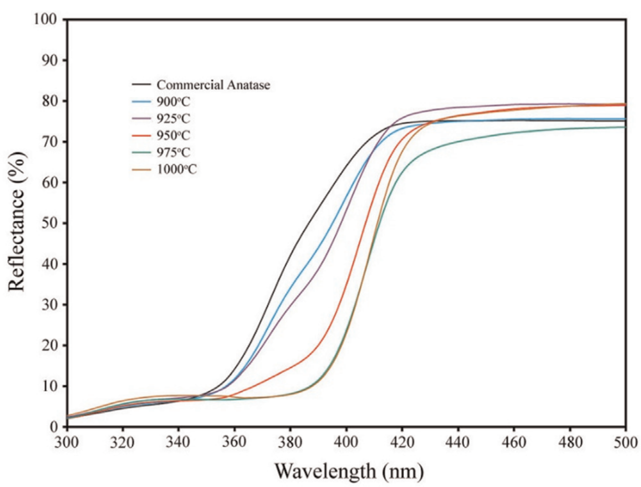


**Fig. 5.** The reflection spectra of the commercial anatase and annealed $TiO_2$ powders as a function of annealing temperature.

Fig. 5 shows the plot of reflection spectra of commercial anatase and annealed particles. The figure shows that commercial anatase can absorb only in UV region. However, the red shift on reflection spectra appeared on the annealed particles. This results annealed particles to be able to absorb the visible light. The band gap of the all samples are shown in Table 1. This data suggests that the band gap decreased with increasing annealing temperature. Since, the band gap of rutile is lower than anatase, therefore the decrease of band gap is the results of anatase–rutile phase transformation.

### 3.2. Photocatalytic activity

The MB removal performance of the commercial anatase and annealed $TiO_2$ powders is presented in Fig. 6. It has to be noted that the photocatalytic activity of $TiO_2$ particles reduced with the increasing annealing temperature. This is due to the differences of $TiO_2$ polymorphs and surface area at different annealing temperature. As reported in other studies [11,14], the photocatalytic activity of $TiO_2$ is affected by a variety of factors. Among of which, polymorphs and specific surface area play the core roles. The $TiO_2$ powders annealed at 900 °C and 925 °C with anatase:rutile ratio of 92:8 and 77:23, respectively, showed the highest activity of ~99% of MB removal. Meanwhile, the performance of the powders annealed from 950 °C to 1000 °C decreased significantly from 65% to 34%. This can be explained by the low specific surface area, large agglomerate size and the high content of rutile phase (>50% of rutile) leading to the high electron–hole recombination rate, which reduces the photocatalytic activity of particles.

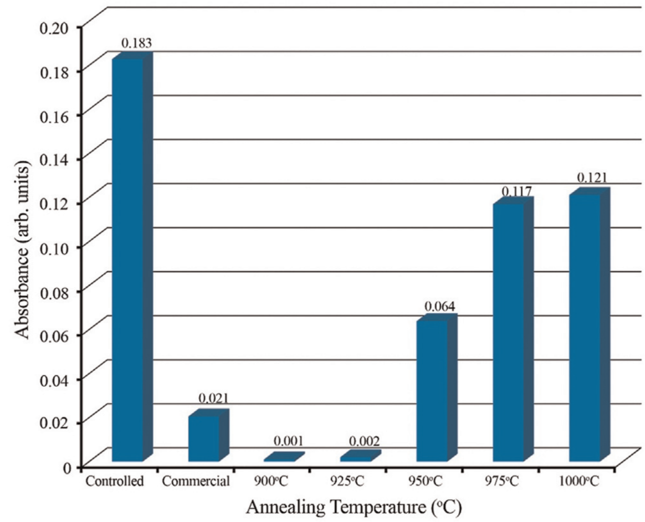


**Fig. 6.** MB removal performance of the commercial anatase and annealed $TiO_2$ powders at different temperatures.

On the other hand, compared to the $TiO_2$ powders annealed at 900 °C and 925 °C, although the commercial anatase has higher anatase portion (96%), smaller agglomerate size (400 nm) and higher specific surface area (~1 $m^2/g$), its activity is lower (89% of MB removal). This is due to the wide band gap of anatase leading to the requirement of high energy source to activate the anatase. Therefore, in this case, because the energy source (UV light 380 nm) may not strong enough to activate anatase easily and thoroughly, the commercial anatase activity is low. These results suggest the leading role of phase composition, which can be controlled by changing annealing temperature, in influencing the photocatalytic activity of $TiO_2$ powders.

## 4. Conclusion

The present work has succeeded in synthesising the mixed phase of anatase and rutile by annealing the commercial anatase in muffle furnace at different temperature, particularly 900, 925, 950, 975, and 1000 °C. The XRD data indicates that the percentage of rutile increases with the annealing temperature and the transformation process almost completed at 1000 °C. In addition, the phase transformation is a linear function of annealing temperature so it is possible to control the phase composition of $TiO_2$ by changing the annealing temperature. The SEM and BET results point out the increase of agglomerate size and the decrease of specific surface area when raising the annealing temperature. This proves that the anatase has smaller agglomerate size and higher surface area compared to rutile. The photocatalytic activity of the annealed $TiO_2$ powders is found to be a function of phase composition. The samples annealed at 900 °C and 925 °C with anatase: rutile ratio of 92:8 and 77:23, respectively, obtained the highest performance of MB removal. In conclusion, the present work suggests that photocatalytic activity of $TiO_2$ powder can be enhanced by changing its phase composition which can be controlled by annealing temperature. In addition, despite the antase/rutile shows a linear trend, in the meantime, the phase ratio effects on other parameter including particle size, agglomerate, surface area, and band gap. These parameters are very important for photocatalytic activity. However, the surface area and band gap should be the most important parameters since both relate to contact area and electron–hole generation, respectively.

## Acknowledgement

The authors would like to thank to Opa Tangpitukkul's Scholarship, Siam Kubota Cooperation Co. Ltd., and Naresuan University's Research Funding for the financial support.

## References

[1] M.S. Liang, C.C. Khaw, C.C. Liu, S.P. Chin, J. Wang, H. Li, Ceram. Int. 39 (2013) 1519–1523.
[2] R.G. Freitas, M.A. Santanna, E.C. Pereira, Electrochim. Acta 136 (2014) 404–411.
[3] K. Murugan, R. Subasri, T.N. Rao, A.S. Gandhi, B.S. Murty, Prog. Org. Coat. 76 (2013) 1756–1760.
[4] K. Nakata, T. Ochiai, T. Murakamia, A. Fujishima, Electrochim. Acta 84 (2012) 103–111.
[5] X. Liu, G. Chen, C. Su, J. Colloid Interface Sci. 363 (2011) 84–91.
[6] Y. Gao, H. Wang, J. Wu, R. Zhao, Y. Lu, B. Xin, Appl. Surf. Sci. 294 (2014) 36–41.
[7] C. Reitz, J. Reinacher, P. Hartmann, T. Brezesinski, Catal. Today 225 (2014) 55–63.
[8] M. Toyoda, Y. Nanbu, Y. Nakazawa, M. Hirano, M. Inagaki, Appl. Catal., B: Environ. 49 (2004) 227–232.
[9] M. Bellardita, A. Di Paola, L. Palmisano, F. Parrino, G. Buscarino, R. Amadelli, Appl. Catal. B: Environ. 104 (2011) 291–299.
[10] N. De la Cruz, R.F. Dantas, J. Giménez, S. Esplugas, Appl. Catal. B: Environ. 130–131 (2013) 249–256.
[11] A.M. Luis, M.C. Neves, M.H. Mendonca, O.C. Monteiro, Mater. Chem. Phys. 125 (2011) 20–25.
[12] S.S. Arbuj, R.R. Hawaldar, U.P. Mulik, B.N. Wani, D.P. Amalnerkar, S. B. Waghmode, Mater. Sci. Eng. B 168 (2010) 90–94.
[13] S. Chin, E. Park, M. Kim, J. Jurng, Powder Technol. 201 (2010) 171–176.
[14] D.C. Hurum, A.G. Agrios, S.E. Crist, K.A. Gray, T. Rajh, M.C. Thurnauer, J. Electron Spectrosc. Relat. Phenom. 150 (2006) 155–163.
[15] A. Kafizas, S. Kellici, J.A. Darr, I.P. Parkin, J. Photochem. Photobiol. A: Chem. 204 (2009) 183–190.
[16] M. Pelaez, N.T. Nolan, S.C. Pillai, M.K. Seery, P. Falaras, A.G. Kontos, P.S. M. Dunlop, J.W.J. Hamilton, J.A. Byrne, K. O'Shea, M.H. Entezari, D.D. Dionysiou, Appl. Catal. B: Environ. 125 (2012) 331–349.
[17] N. Wetchakun, B. Incessungvorn, K. Wetchakun, S. Phanichphant, Mater. Lett. 82 (2012) 195–198.
[18] A. Nakaruk, D. Ragazzon, C.C. Sorrell, Thin Solid Films 518 (2010) 3735–3742.
[19] J. Tauc, A. Menth, J. Non Cryst. Solids 8–10 (1972) 569–585.
[20] A. Mills, J. Wang, J. Photochem. Photobiol. A: Chem. 127 (1999) 123–134.
[21] A. Nakaruk, G. Kavei, C.C. Sorrell, Mater. Lett. 64 (2010) 1365–1368.
[22] C.R. Hubbard, E.H. Evans, D.K. Smith, J. Appl. Cryst. 9 (1976) 169–174.
[23] D.A.H. Hanaor, C.C. Sorrell, J. Mater. Sci. 46 (2011) 855–874.